JOURNAL OF GEOPHYSICAL RESEARCH, VOL. 102, NO. A11, PAGES 24,333–24,338, NOVEMBER 1, 1997

Long lasting energetic proton precipitation in the inner magnetosphere after substorms

B. B. Gvozdevsky

Polar Geophysical Institute, Apatity, Russia

V. A. Sergeev

Institute of Physics, University of St. Petersburg, St. Petersburg, Russia

K. Mursula

Department of Physical Sciences, University of Oulu, Oulu, Finland

Abstract. Data of polar-orbiting low-altitude NOAA spacecraft are used to study the precipitation of energetic (30-80 keV) protons, several degrees equatorward of the energetic proton isotropic boundary. This precipitation, to be called low-latitude proton precipitation (LLPP), is observed at all local time sectors. The LLPP precipitating flux is found to be generally smaller than the trapped flux. The LLPP particle flux significantly increases during intense substorms and then decays with a long characteristic timescale of about 9 hours. Therefore, it may also be found during very quiet times. The long decay and the observed loss cone anisotropy imply a moderate pitch angle diffusion of energetic protons. During quiet magnetic conditions following the disturbance the latitudinal position of the LLPP region moves slowly to higher latitudes. The equatorial boundary of the precipitation is found to be at lower latitudes in the night sector than in the dayside sector. Mapping to the equatorial plane along magnetic field lines showed that the equatorial boundary of the precipitation at the nightside is situated on a closer drift shell than that at the dayside.

1. Introduction

When studying the ratio of trapped and precipitating fluxes of energetic protons measured by low-altitude spacecraft, one usually observes a very simple anisotropy pattern (see Figure 1a). As a spacecraft crosses the auroral zone from high to low latitudes, it first detects an isotropic flux distribution. Then the flux within the loss cone drops, while the flux of trapped particles continues to be high in the radiation belt at lower latitudes. The boundary between zones of isotropic and anisotropic fluxes is called the isotropic boundary (IB). It has been shown earlier [*Sergeev et al.*, 1983, 1993] that the isotropic flux is caused by pitch angle scattering in the equatorial current sheet, where, because of the large curvature of magnetic field lines, the first adiabatic invariant is violated, and particles are effectively scattered into the loss cone. Closer to the Earth (at lower latitudes for a low-altitude spacecraft) the field lines are more dipolar, and the particle motion is more adiabatic. Therefore the loss cone is almost empty, unless significant plasma turbulence exists.

Sometimes, however, a region of rather intense proton precipitation is observed equatorward of the IB (see Figure 1b). Typically, the particle flux here is not completely isotropic (i.e., $J_{\parallel}/J_{\perp} < 1$). Hereafter we refer to such a region as the low-latitude proton precipitation (LLPP) region. Sometimes the LLPP is separated from the isotropic zone by an intermediate region with very low precipitation.

Paper number 97JA02062.
0148-0227/97/97JA-02062$09.00

The LLPP region has earlier been explored in cases of proton energies of a few keV and about 100 keV on the basis of data from the ESRO 1A spacecraft [e.g., *Hauge and Søraas*, 1975; *Hultqvist*, 1975; *Søraas et al.*, 1977; *Lundblad et al.*, 1979]. It was also found in the equatorial magnetosphere by *Williams and Lyons* [1974], who, on the basis of data from the Explorer 45 spacecraft, studied the pitch angle distributions of ~1 keV to several hundred keV protons during the storm recovery phase.

In spite of earlier research, many features of the LLPP are not well understood, and some results, for example, concerning on its local time dependence and relationship with magnetic activity, are conflicting. *Hauge and Søraas* [1975] studied the precipitation of >115 keV protons in the evening and forenoon sectors and its relation to magnetic activity. They showed that the properties of the LLPP region (they called it "a drizzle zone") in the evening and forenoon sectors are quite different, implying a significant LT dependence. These authors also found that "the intensity of the drizzle in the evening sector seems to be rather independent of the instantaneous magnetic activity, except for cases where the main zone of auroral protons moves equatorwards, overlapping the drizzle zone." (The equatorward expansion of the isotropic zone takes place during geomagnetic disturbances.) The dynamical features of the >100 keV proton precipitation during different phases of substorms have been also studied by *Lundblad et al.* [1979]. They found that the low-latitude anisotropic precipitation zone is remarkably stable during substorms. They did not mention any significant local time variations in the characteristics of this zone. Whereas previous authors seem to infer only a small sensitivity of the LLPP to the magnetic activity, *Sanchez et al.* [1993] used DMSP observations of <30 keV protons and found a specific precipitation lo-

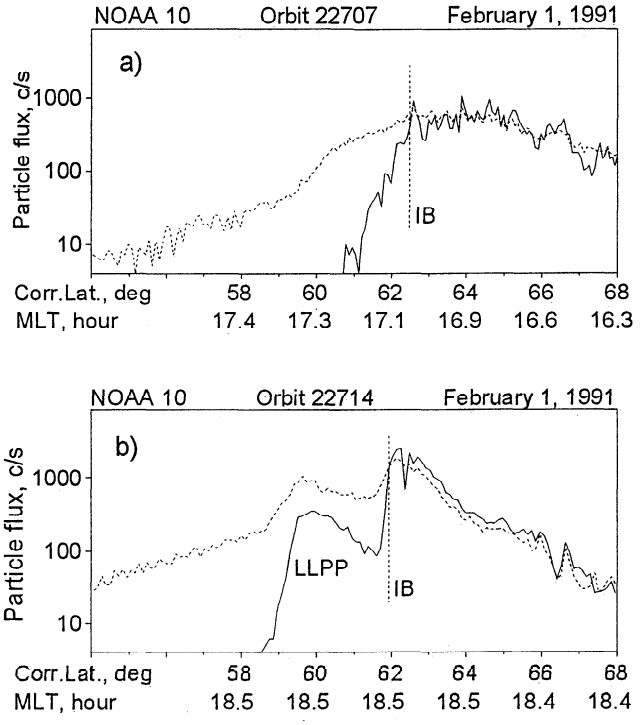

Figure 1. Examples of energetic proton fluxes (solid line, precipitating flux; dashed line, trapped flux) observed by NOAA spacecraft: (a) the usual pattern with a sharp decrease of the precipitating flux equatorward of the isotropic boundary; (b) pattern with a distinct low-latitude proton precipitation region.

cated equatorward of (and detached from) the main body of proton precipitation, which appears shortly after intense substorms. This precipitation was found mainly in the midnight and dusk local time sectors.

Besides the somewhat conflicting statements on the activity and LT dependence of the LLPP, little is also known about the possible sources of the LLPP and its precipitation mechanisms. *Sanchez et al.* [1993] have found that particles inside this region have a spectrum similar to the plasma sheet ion spectrum, suggesting a plasma sheet origin of the LLPP. *Williams and Lyons* [1974] have shown the existence of an inner region of moderate anisotropy (possible equatorial extension of the LLPP) which was separated from the outer isotropic region by a zone in which the proton loss cone was empty. They argued that the inner region is situated at the plasmapause and is caused by ion cyclotron waves. *Lundblad and Søraas* [1978] interpreted the spatial coincidence of the low-latitude anisotropic proton precipitation and the stable auroral red (SAR) arc to be due to ion cyclotron waves producing both the precipitation and the arc. Several other proton precipitation mechanisms have been discussed in the literature, including scattering by lower hybrid waves [*Roth et al.*, 1990], Pc 5 waves [*Li et al.*, 1993], plasmaspheric hiss [*Kozyra et al.*, 1994], and whistler waves [*Villalon and Burke*, 1994]. A careful investigation of the LLPP morphology is clearly required in order to distinguish the dominant mechanism among the several candidates.

The purpose of our work is to clarify the so far conflicting aspects of the LLPP morphology, including its relation to magnetic activity, its temporal characteristics and local time variation. We also investigate its spatial distribution, mapping it into the equatorial magnetosphere in order to infer the physical parameters in the source region of the LLPP.

2. Observations

2.1. Available Data and Examples of Low-Latitude Proton Precipitation

To study the proton precipitation, we used data from the low-altitude polar-orbiting NOAA spacecraft TIROS-N and NOAA 6 (in August 1979) as well as NOAA 10 (in January and February 1991). All satellites of this series include similar instruments to measure the directional flux of 30-80 keV protons in two perpendicular directions, one channel measuring the precipitating flux (pitch angles inside the loss cone at high latitudes) and the other measuring the locally trapped flux (pitch angles close to 90°). In the figures the flux unit is counts per second (c/s). When converting these values to the directional number flux, one must divide them by the instrument's geometric factor, which is 0.0095 cm^2 sr. The spacecraft altitude is about 850 km. The time resolution of the instrument is 2 s. For more information about the spacecraft and the instruments, see *Hill et al.* [1985].

Figure 1 shows typical flux distributions of energetic protons observed during a spacecraft crossing of the auroral zone. Solid lines represent the precipitating flux, and dashed lines denote the trapped particles. The isotropic precipitation occupies the poleward part of the precipitation region, poleward of the IB. In Figure 1a the precipitating flux drops fairly sharply equatorward of the IB. Figure 1b shows a different pattern. Equatorward of the IB one can still observe a region of intense precipitation (the LLPP region). Usually, the precipitating flux is less than the trapped flux within this region, but occasionally, a full isotropization can be observed. The LLPP either is separated from the main precipitation by a zone of depleted flux, as in Figure 1b, or looks like a low-latitude "shoulder" attached to the main body of isotropic precipitation. When identifying a region of equatorward anisotropic precipitation as an LLPP, we imposed the following criteria in our study. First, the maximum precipitating flux within this region must exceed 5 c/s in order to be distinguished from background noise. Second, either the latitudinal width of the region must exceed 2° at the level 5 c/s, or the region must be separated from the main isotropic precipitation by a zone of diminished precipitation (as in Figure 1b), the minimum flux in the separation zone being less than half the maximum LLPP flux. The equatorward boundary of the LLPP is typically sharp, the precipitating flux decreasing by 1 order of magnitude within 1° of latitude. Figure 1b presents an evening pass of the satellite, but other local time sectors show qualitatively the same profile.

2.2. Relationship Between Magnetic Activity and Temporal Characteristics

To study the long-term evolution of LLPPs, we counted the daily number of cases in which the NOAA 6 and TIROS-N spacecraft observed well-defined LLPP regions during 20 days in August 1979. Orbits of these two spacecraft were almost perpendicular to each other at polar latitudes. Moreover, the orbits were displaced considerably in magnetic coordinates. Thus the two spacecraft covered all local time sectors in the auroral zone. Figure 2 shows the number of daily LLPP observations compared with indices of geomagnetic activity. The number of observed LLPPs is distinctly increased during the days following an intense geomagnetic disturbance, including some very quiet days.

Next we selected three intense substorms followed by long quiet periods: August 13-15, 1979, and January 23-25 and February 1-3, 1991. These three events can also be classified as

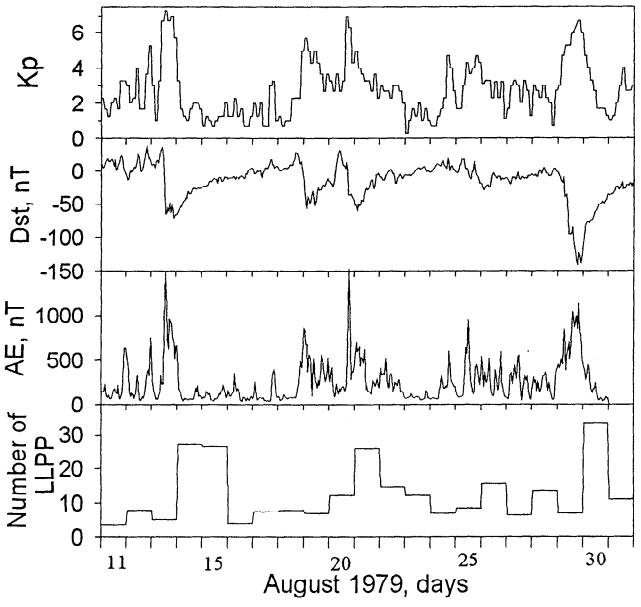

Figure 2. Geomagnetic activity indices (*Kp, Dst,* and *AE*) and daily numbers of the LLPPs observed by NOAA 6 and TIROS-N spacecraft in August 1979.

weak to moderate geomagnetic storms, as large substorms also produce *Dst* variations. The selected substorms are fairly isolated disturbances; i.e., there are prolonged quiet periods both before and after the disturbance. This condition ensures that the effect of any preceding disturbances is minimized and guarantees that the observed particle population was born in the course of the given substorm. Figures 3a-3c present a summary of the geomagnetic activity indices and the intensity of the detected LLPPs for these three periods. Each point represents the maximum precipitating flux within one LLPP region sampled during a satellite pass in the night sector (1900-0500 magnetic local time, or MLT).

All three cases depicted in Figures 3a-3c demonstrate that the intensity of the LLPP increases during a substorm and then gradually declines during the quiet period following the disturbance. The characteristic time constant (*e*-folding time) of the intensity decrease is rather large, about 11, 7, and 9 hours, as calculated for August 14-15, 1979, January 24-25, 1991, and February 2-3, 1991, respectively. Hereafter we will call this characteristic decay time the lifetime. (We note that the decrease may not be exactly exponential. The longer the quiet interval we consider, the longer lifetime is obtained. This is one reason the lifetime estimates from the three sample cases in Figures 3a-3c differ). The long lifetime of the LLPP precipitation is consistent with the results of our survey shown in Figure 2. Although it is not shown in Figure 3, the locally trapped flux also declines during the quiet period at the same rate as the precipitating flux. Precipitating to trapped flux ratio $J_{||}/J_{\perp}$ (not depicted) does not show any clear trend, and the scatter of points is rather big, varying between 0.1 and 1. This scatter may be caused by several factors, such as the dependence of the precipitating to trapped flux ratio on MLT or on geographic longitude: particle fluxes vary with longitude, since the mirroring height depends on it. (This effect was studied among others by *Berg and Søraas* [1972]. Accordingly, these effects may mask a possible real variation of the ratio $J_{||}/J_{\perp}$ with time after the substorm.

Figures 3a-3c also demonstrate that the latitude of the maximum LLPP flux decreases during the substorm and then increases during the following quiet period. The increase is gradual in Figures 3a and 3c, but in Figure 3b the latitude increases sharply immediately after the disturbance and then stays approximately at a constant level. In Figure 3a one can see some tendency of the decay rate to be larger (and the lifetime shorter) at lower latitude: the slope of intensity decrease is somewhat steeper in the beginning of the quiet period when LLPP is observed at lower latitudes than at the end of it at slightly higher latitudes. However, such a dependence is not very pronounced, and the shorter periods (Figures 3b and 3c) do not show this dependence at all.

Note that Figure 3b shows only a few recognized LLPP samples before and at the beginning of the substorm and that the LLPP fluxes are fairly low during that time. This effect is due to the rather quiet conditions during 3 days preceding January 23, when the *AE* index did not exceed 250 nT. Figure 3c presents a different situation. The preceding day, January 31, was more disturbed with the *AE* index exceeding 600 nT. As a result, the LLPP was well registered almost on each satellite pass and had a rather high intensity even before the substorm. (The gap on the plot of LLPP flux at the end of February 2 is due to the absence of data.) Sometimes even during a substorm we could not recognize the LLPP. For example, in Figure 3b there are only a few LLPP points by the end of the substorm. However, as we will discuss later in section 3, this lack of data does not necessarily mean that the LLPP is absent during that time.

2.3. Local Time Dependence

An important morphological characteristic is the magnetic local time distribution of the precipitation intensity. We demonstrate this distribution for the quiet period of August 14-15, 1979, when data from two spacecraft (NOAA 6 and TIROS-N) were available to cover most local time sectors of the auroral zone. Other studied events show a similar picture. The magnetic local time distribution of the maximum LLPP precipitating flux is shown in Figure 4. Data sampled from both hemispheres are included. Solid circles denote the data of August 14, and open circles denote the data of August 15. Figure 4a demonstrates the maximum intensity of the LLPP precipitation versus MLT. The scatter of points is rather large, especially during day hours. Again, one of the factors contributing to this scatter may be the diurnal variation of the flux level due to the dependence of the mirroring height on geographic longitude. Despite the large scatter, Figure 4a shows a clear variation of the flux level on MLT with a flux maximum at midnight and a flux decrease from the nightside toward the dayside. To better depict this dependence in Figure 4a, we indicated the median flux values of each 2-hour bin on August 14 by horizontal dashes. Also, one can see in Figure 4a the lower LLPP intensity during night hours of August 15 in comparison with those of August 14. This decrease was already seen in Figure 3a. At dayside such a decrease is not observed.

Figure 4b depicts the (corrected geomagnetic) latitude of the maximum flux of each LLPP region as a function of MLT. As can be seen, the LLPP is observed at higher latitudes at the dayside. The pattern is almost symmetric around the noon-midnight line. Open circles, corresponding to August 15, lie about 1° higher than solid circles (August 14) during night hours. This poleward motion of the LLPP maximum during the quiet period after the disturbance can be clearly seen also on the lowest panel of Figure 3a. At the dayside this shift is not observed. Again the scatter of points is larger at the dayside.

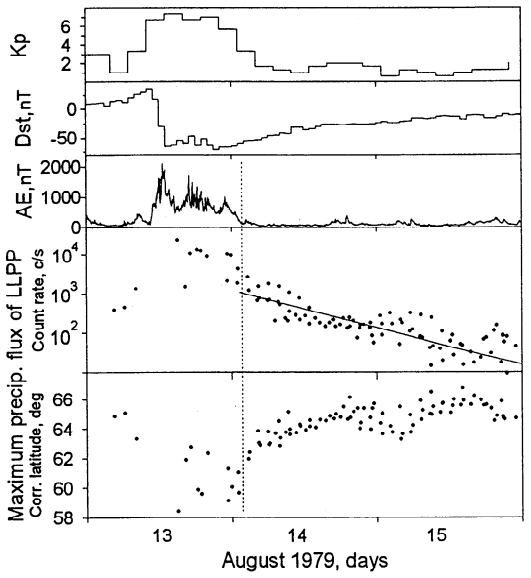

Figure 3a. Geomagnetic activity indices, maximum precipitating flux within each LLPP region, and the corrected geomagnetic latitude of this maximum during August 13-15, 1979. Points are sampled only at the night sector (1900-0500 MLT).

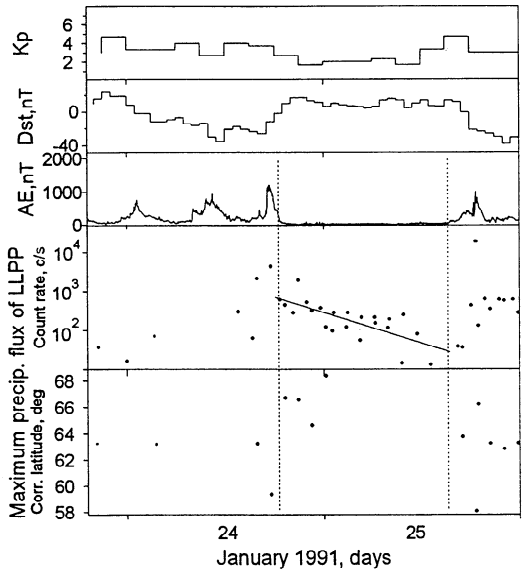

Figure 3b. Same as in Figure 3a for January 23-25, 1991.

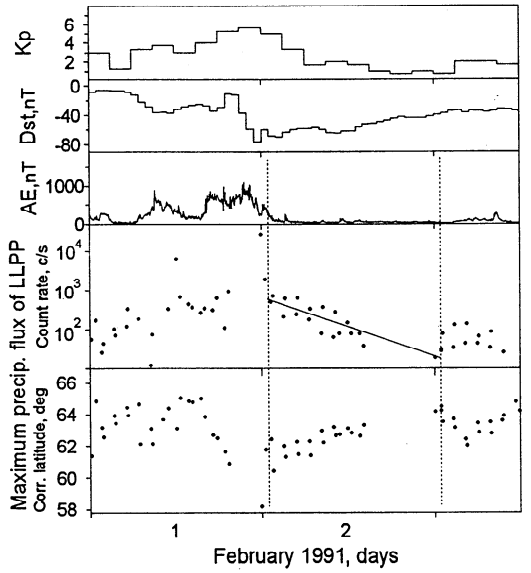

Figure 3c. Same as in Figure 3a for February 1-3, 1991.

2.4. Mapping to the Equatorial Plane

To obtain information on the equatorial source region of the LLPP, we mapped its equatorward boundary into the equatorial plane along the magnetic field lines. As the magnetic configuration undergoes significant changes during active periods, a more accurate mapping is obtained during quiet periods. We used Tsyganenko's magnetospheric model T89 for mapping. The choice of the best variant of the model was made by using the Isotropic Boundary Algorithm (previously described and tested by *Sergeev et al.*, [1993]. This algorithm is based on the fact that the position of the isotropic boundary of energetic particles is determined mainly by the magnetic field in the near-equatorial region. So we chose the variant of the T89 model that gave isotropic boundary positions closest to the observed ones.

Figure 5 shows the equatorial projection of the equatorward boundaries of the LLPPs registered during the quiet periods on August 14-15, 1979. Points mapped from both hemispheres are included. During this period, two spacecraft were in orbit and covered most local time sectors. Solid circles in Figure 5 denote August 14 data, while open circles correspond to August 15. A small shift outward, away from the Earth at the nightside, is visible in Figure 5. (The same trend was also seen in Figure 4b.) Solid lines in Figure 5 present the drift shells of ~0° pitch angle particles computed from the magnetospheric model by assuming that the first and second adiabatic invariants are conserved. One can note that at the night sector the LLPP equatorward boundaries lie close to one drift shell. However, further out from midnight the boundaries are observed on more distant shells. The radial equatorial distance of the LLPP varies from about 4.5 R_E at midnight to about 5.5 R_E at noon. The corresponding values of the model magnetic field are ~350 nT at midnight and ~200 nT at noon.

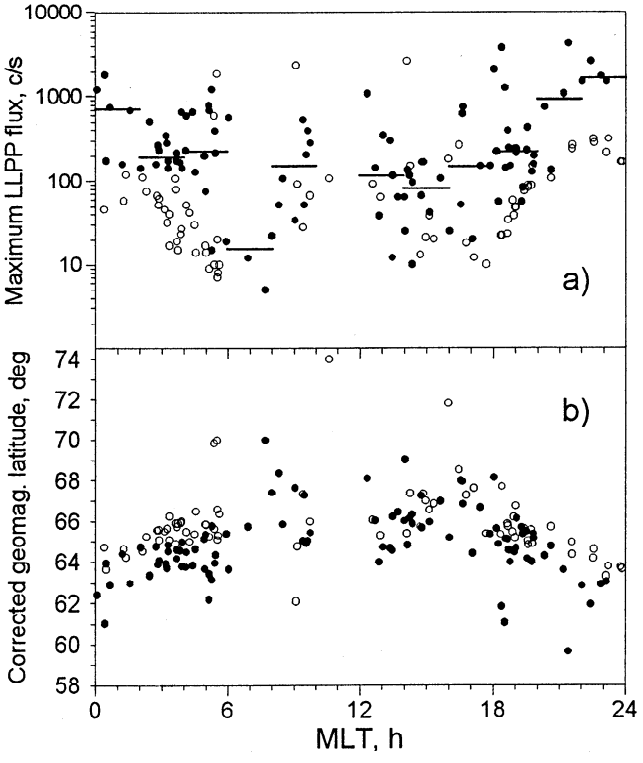

Figure 4. Magnetic local time distribution of (a) the LLPP maximum precipitating flux and (b) its latitudinal position, for the period of August 14 (solid circles) and 15 (open circles), 1979. Dashes in Figure 4a denote median values for each 2-hour bin on August 14.

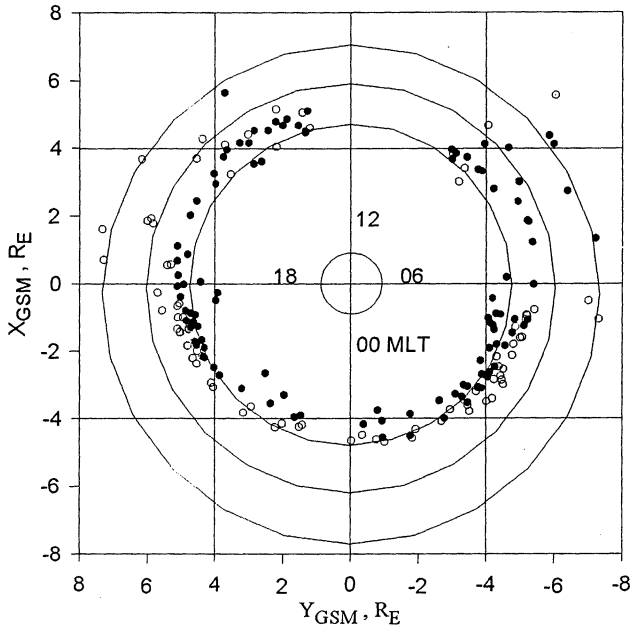

Figure 5. Equatorial projection of the drift shells of ~0° pitch angle particles and the LLPP equatorward boundary (solid circles, August 14; open circles, August 15, 1979).

3. Discussion and Conclusion

We have investigated the low-latitude precipitation of energetic (E = 30-80 keV) protons (the so-called LLPP region), which is observed equatorward of the main isotropic precipitation zone. The most important property of the LLPP is the moderate rate of the pitch angle diffusion in this region. Following the estimate of the characteristic lifetime of particles in the limit of strong pitch angle diffusion [*Kennel*, 1969], $\tau = T_b/2\alpha^2$, and taking for 30 keV protons the bounce period $T_b \approx 1$ min and the equatorial loss cone $\alpha \approx 0.055$ at L=5 ($\alpha \approx \sqrt{(B_{eq}/B_{ionosph})}$; $B_{eq} \approx$ 210 nT, $B_{ionosph} \approx$ 48,000 nT), we obtain $\tau \approx 2$ hours. Our observations gave a larger proton lifetime (characteristic decay time) of about 9 hours. Together with the fact that the observed fluxes had a considerable anisotropy (typically $J_{||}/J_{\perp} \sim 0.1$), this finding implies that the pitch angle diffusion rate was only moderate. If we take into account that the proton drift period is about 5 hours, the protons in the LLPP region can perform several complete revolutions drifting around the Earth. This fact should be taken into account in discussing the mechanisms of LLPP precipitation.

The observed long lifetime can explain the conflicting statements about the relationship between the LLPP and magnetic activity in previous studies. The times during which the LLPP intensity increases considerably correlate well with the intense substorms or magnetic storms (see statistics in Figure 2 and events in Figure 3). However, because of their long lifetime the protons may continue to precipitate in the LLPP region during a couple of days after the LLPP was generated, and they may be observed even during very quiet days.

According to *Williams and Lyons* [1974] and *Søraas et al.* [1977], between the high-latitude isotropic precipitation and the low-latitude region of moderately weak precipitation there is a zone of highly anisotropic pitch angle distribution with almost no protons in the loss cone. *Søraas et al.* [1977] noticed that this zone tends to be wider and more pronounced for 1-6 keV than for 100 keV protons. In this study we dealt with high-energy (30-80 keV) protons. Probably for this reason we most often did not observe a clear gap between the LLPP and the isotropic boundary; i.e., the majority of events were of the "shoulder" type. Moreover, *Williams and Lyons* [1974] mentioned that during the main phase of a magnetic storm and after prolonged quiet periods it may be that the inner and outer precipitation regions are contiguous. Therefore the gap between the inner and outer precipitation exists during a relatively short time after a storm.

In section 2.2 we mentioned that sometimes during a substorm maximum epoch we could not recognize the LLPP. There may be two reasons for this failure. First, in the course of a substorm, isotropic plasma is injected into the inner magnetosphere. As a consequence of such an injection a region of low-latitude precipitation appears, but using our formal criteria for identifying the LLPP, we may not be able to recognize it if a fully isotropic flux is observed both in this region and in the high-latitude isotropic zone. So it may be impossible to distinguish between the two regions. The second possible reason is the equatorward motion of the isotropic boundary during disturbed times. This displacement was shown among others by *Hauge and Søraas* [1975, Figures 2 and 3], *Hultqvist* [1975, Figure 19c], *Imhof et al.* [1979, Figures 7a and 7b], and *Sergeev and Gvozdevsky* [1995, Table 1]. When the IB moves equatorword, the isotropic zone can completely overlap the LLPP region, making it invisible. After the substorm the precipitating flux gradually declines and/or the IB returns to higher latitudes, and the LLPP region becomes distinguishable. (We note that the two processes mentioned above are different. While the first process is related to the intensity of the low-latitude precipitation regardless the IB position, the second one is caused by field line stretching. When the magnetotail becomes more stretched, all projections to the ionosphere, including both IB and LLPP, move equatorward simultaneously. But the IB moves further equatorward for another reason, namely, because the point of the critical curvature of field lines in the equatorial plane moves closer to the Earth.)

The LLPP latitude profiles at different local times look fairly similar, and they have a rather well defined equatorial boundary. The origin of this boundary may also have different explanations. First, we may connect this boundary with the process of inward plasma injection during the substorm, if there exists some inner boundary for earthward plasma penetration. In that case the LLPP equatorward boundary should approximately coincide with the magnetic drift shell (at least after about 5 hours required for the 30 keV protons at L~5 to complete their azimuthal drift). Our mapping results (Figure 5) show, however, that this suggestion may only be true in the nightside and is obviously violated in the dayside sector, where the mapped LLPP boundary appears much further out in comparison with the drift shell passing through the LLPP boundary at nightside. This finding implies that some loss process affects the formation of the equatorward boundary.

Plasmapause may be a candidate to form a sharp boundary, because it separates the region of dense (plasmasphere) and dilute (outer radiation belt) plasma. High plasmaspheric density may influence the excitation of plasma turbulence, resulting in particle scattering and precipitation. The location of the LLPP boundary at L~5 in the night sector favors this hypothesis, since this is quite a reasonable distance for the plasmapause during low activity conditions. Moreover, the outward displacement of the LLPP during a quiet period may be related to the plasmasphere refilling after substorm. But there are also some arguments against the plasmasphere as a cause of the precipitation

and against the plasmapause as the cause of formation of the LLPP equatorward boundary. First, the high plasmaspheric density typically favors a larger growth of plasma instabilities [*Williams and Lyons*, 1974]. In that case the plasmapause may correspond to the outer boundary of precipitation, rather than to its inward (equatorward) boundary. Second, the plasmasphere is expected to have a pronounced bulge in the evening sector. In Figure 5 the LLPP inner boundaries show some tendency to a bulge in the eveningside. However, this bulge is not very pronounced, and moreover, the same tendency is seen in the morningside, which cannot be explained by the plasmasphere.

Concluding the discussion, we summarize our results as follows. We have investigated the low-latitude precipitation of energetic (E = 30-80 keV) protons, which is observed equatorward of the main isotropic precipitation zone. We found that the LLPP is generated during intense substorms and that its intensity decays with a long characteristic timescale of about 9 hours due to only moderate pitch angle diffusion of particles into the loss cone. We did not find a very clear local time asymmetry of the LLPP intensity. We showed a pronounced local time variation of the LLPP equatorward boundary latitude and found a slow shift of its position with time (~1° per day) during quiet magnetic conditions. Mapping the LLPP boundary to the equatorial plane during prolonged quiet periods set its location at L ~ 4.5 at the nightside, in the equatorial magnetic field of about 350 nT. At the dayside this boundary is located outward of this drift shell at L ~ 5.5, in the magnetic field of about 200 nT. The origin of the LLPP and of its equatorward boundary was discussed, and several candidates were presented. However, further studies are required to settle the remaining open questions.

Acknowledgments. NOAA spacecraft data were made available through the WDC-A for STP (Boulder). B. Gvozdevsky and V. Sergeev thank the International Science Foundation for financial support (under grant NWT000) and the staff of the Department of Physical Sciences of University of Oulu for their hospitality during stays in Oulu. Furthermore, financial support from the Centre for International Mobility (CIMO), Finland, is gratefully acknowledged.

The editor thanks two referees for their assistance in evaluating this paper.

References

Berg, L. E., and F. Søraas, Observations suggesting weak pitch angle diffusion of protons, *J. Geophys. Res., 77,* 6708, 1972.

Hauge, R., and F. Søraas, Precipitation of >115 keV protons in the evening and forenoon sectors in relation to the magnetic activity, *Planet. Space Sci., 23,* 1141, 1975.

Hill, V. J., D. S. Evans, and H. H. Sauer, TIROS/NOAA satellites space environment monitor: Archive tape documentation, *NOAA Tech. Memo. ERL SEL-71*, Environ. Res. Lab., Boulder, Colo., 1985.

Hultqvist, B., The ring current and particle precipitation near the plasmapause, *Ann. Geophys., 31*, 111, 1975.

Imhof, W. L., J. B. Reagan, and E. E. Gaines, Studies of the sharply defined L dependent energy threshold for isotropy at the midnight trapping boundary, *J. Geophys. Res., 84,* 6371, 1979.

Kennel, C. F., Consequences of a magnetospheric plasma, *Rev. Geophys., 7,* 379, 1969.

Kozyra, J. U., C. E. Rasmussen, and L. R. Lyons, The interaction of ring current and radiation belt protons with ducted plasmaspheric hiss, 1, Diffusion coefficients and time scales, *J. Geophys. Res., 99,* 4069, 1994.

Li, X., M. Hudson, A. Chan, and I. Roth, Loss of the ring current O$^+$ ions due to interaction with Pc 5 waves, *J. Geophys. Res., 98,* 215, 1993.

Lundblad, J. Å., and F. Søraas, Proton observations supporting the ion cyclotron wave heating theory of SAR arc formation, *Planet. Space Sci., 26,* 245-254, 1978.

Lundblad, J. Å., F. Søraas, and K. Aarsnes, Substorm morphology of >100 keV protons, *Planet. Space Sci., 27,* 841, 1979.

Roth, I., B. I. Cohen, and M. K. Hudson, Lower hybrid drift instability at the inner edge of the ring current, *J. Geophys. Res.*, 95, *3,* 2325, 1990.

Sanchez, E. R., B. H. Mauk, P. T. Newell, and C.-I. Meng, Low-altitude observation of the evolution of substorm injection boundary, *J. Geophys. Res., 98,* 5815, 1993.

Sergeev, V. A., and B. B. Gvozdevsky, MT-index: A possible new index to characterize the magnetic configuration of magnetotail, *Ann. Geophys., 13,* 1093, 1995.

Sergeev, V. A., E. M. Sazhina, N. A. Tsyganenko, J. Å. Lundblad, and F. Søraas. Pitch-angle scattering of energetic protons in the magnetotail current sheet as the dominant source of their isotropic precipitation into the nightside ionosphere, *Planet. Space Sci., 31,* 1147, 1983.

Sergeev, V. A., M. V. Malkov, and K. Mursula, Testing of the Isotropic Boundary Algorithm method to evaluate the magnetic field configuration in the tail, *J. Geophys. Res., 98,* 7609, 1993.

Søraas, F., J. Å. Lundblad, and B. Hultqvist, On the energy dependence of the ring current proton precipitation, *Planet. Space Sci., 25,* 757, 1977.

Villalon, E., and W. J. Burke, Diffusion of radiation belt protons by whistler waves, *J. Geophys. Res., 99,* 21,329, 1994.

Williams, D. J., and L. R. Lyons, The proton ring current and its interaction with the plasmapause: Storm recovery phase, *J. Geophys. Res., 79,* 4195, 1974.

B. B. Gvozdevsky, Polar Geophysical Institute, Apatity, 184200, Russia. (e-mail: gvoy@pgi-ksc.murmansk.su)

K. Mursula, Department of Physical Sciences, University of Oulu, P.O.Box 333, FIN-90571 Oulu, Finland. (e-mail: Kalevi.Mursula@oulu.fi)

V. A. Sergeev, Institute of Physics, University of St. Petersburg, St. Petersburg, 198904, Russia. (e-mail: sergeev@solar.phys.lgu.spb.su)

(Received May 28, 1996; revised July 10, 1997;
accepted July 16, 1997.)